Spatial and temporal mapping of Al and AlO during oxidation in pulsed laser ablation of $LaAlO_3$

2013 JINST 8 C10021

(http://iopscience.iop.org/1748-0221/8/10/C10021)

PUBLISHED BY IOP PUBLISHING FOR SISSA MEDIALAB

RECEIVED: *September 13, 2013*
ACCEPTED: *October 12, 2013*
PUBLISHED: *October 29, 2013*

16th INTERNATIONAL SYMPOSIUM ON LASER-AIDED PLASMA DIAGNOSTICS,
22–26 SEPTEMBER 2013,
MADISON, WISCONSIN, U.S.A.

Spatial and temporal mapping of Al and AlO during oxidation in pulsed laser ablation of $LaAlO_3$

K. Orsel,[a,1] **R. Groenen,**[b] **H.M.J. Bastiaens,**[a] **G. Koster,**[b] **G. Rijnders**[b] **and K.-J. Boller**[a]

[a]*Laser Physics and Nonlinear Optics, Dept. Science and Technology, MESA+ Research Institute for Nanotechnology, University of Twente, P.O. Box 217, 7500 AE Enschede, The Netherlands*
[b]*Inorganic Material Science, Dept. Science and Technology, MESA+ Research Institute for Nanotechnology, University of Twente, P.O. Box 217, 7500 AE Enschede, The Netherlands*

E-mail: k.orsel@utwente.nl

ABSTRACT: We present the first spatio-temporal mapping of two simultaneously present species in a plasma used for pulsed laser deposition. We apply laser induced fluorescence spectroscopy (LIF) to map ground state populations of Al and AlO in plasma plumes generated by ablation of $LaAlO_3$ in an O_2 or Ar atmosphere. Around a specific distance from the target, we observe Al vanish simultaneously with the turnup of AlO. This can be assigned to the oxidation of Al in the background atmosphere occurring after a sufficient slowing of the expanding Al front. This is consistent with the absence of such effects when argon is taken as background. A quantitative evaluation of data promises to reveal important dynamical reaction and deposition parameters for identification of the origin of specific properties of PLD grown films such as 2-dimensional conductive interfaces.

KEYWORDS: Plasma diagnostics - charged-particle spectroscopy; Plasma diagnostics - interferometry, spectroscopy and imaging

[1]Corresponding author.

doi:10.1088/1748-0221/8/10/C10021

Contents

2013 JINST 8 C10021

1 Introduction

Pulsed Laser Deposition (PLD) is a versatile technique to grow thin films through the deposition of laser ablated material. It allows for the growth of complex materials, like high-temperature superconductors, oxide based ferroelectrics and piezoelectrics [1]. Recently, also film stacks with atomic sharp interfaces are grown which exhibit intriguing properties. One such structure receiving significant attention lately is a thin film oxide heterostructure formed by deposition of $LaAlO_3$ (LAO) on a $SrTiO_3$ (STO) substrate. Ohtomo et al. discovered a high concentration of charge carriers with high mobility confined to the interface of LAO and STO, referred to as a two-dimensional electron gas (2DEG) [2]. These 2DEGs have since been extensively researched [3] and several additional features of the interface have been observed, including superconductivity [4] and magnetism [5].

To explain the high conductivity at the LAO/STO interface, several possible mechanisms have been proposed. These include the creation of oxygen vacancies in the STO substrate resulting from the diffusion of oxygen from the STO to the LAO film which is not fully oxidized. Kalabukhov et al. showed that indeed oxygen vacancies were formed when an LAO film was grown at low oxygen pressures (10^{-6} mbar) [6] caused possibly by an incomplete oxidation of La and Al in the plasma plume [7, 8]. In search for a better understanding and control of the 2DEG, the influence of the PLD parameters, such as background gas and pressure, and laser fluence, on the conductivity at the interface has been studied extensively [3].

However, this empiric approach does not provide direct insight in the oxidation state of the material flux propagating towards the substrate and the influence on the growth of the LAO film. For this, different methods are needed that allow a direct spatial and temporal mapping of the density and flow of the involved species towards the substrate. Of central interest is that chemical reactions become displayed and quantified, such as the dynamics of oxidation, which requires the simultaneous mapping of at least two species.

In an attempt to relate film growth to the material flux in the plasma plume, optical emission spectroscopy (OES) has been used. However, only excited particles that also fluoresce are accessible with this diagnostic method [9–11]. This is a large drawback, because the populations in the excited states are orders of magnitude lower than the ground state populations when the plume has expanded close to the substrate [12]. This means that signals are weak at times beyond the

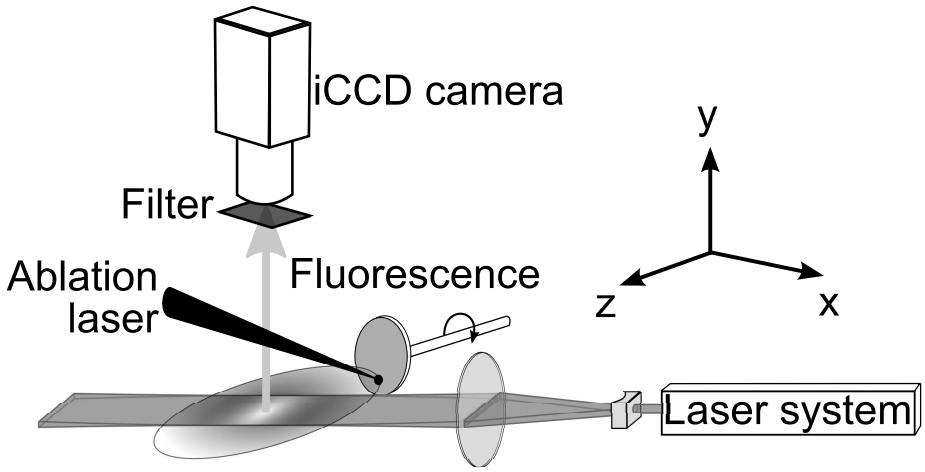

Figure 1. Schematic of the setup. The ablation laser is a KrF laser. The laser system used for the LIF measurements consists of a Nd:YAG laser pumped dye laser with second harmonic generation. The combination of a cylindrical and spherical lens is used to both expand and focus the laser beam in the plane of expansion of the plasma plume. The LIF sheet is set at a 45° angle with the z-axis. Fluorescence is detected through appropriate optical filters with an intensified CCD camera.

fluorescence lifetime and only qualitative and limited information can be gained. However, laser induced fluorescence (LIF) allows a direct spatial and temporal mapping of the density and flow of the involved species towards the substrate [13–15].

In this paper, we report for the first time the spatial and temporal mapping of two species simultaneously, namely aluminum and aluminum oxide, which are related through a chemical reaction in the pulsed laser ablation plasma of $LaAlO_3$.

2 Experimental setup and methodology

The LIF measurements are carried out in a custom built PLD chamber (Twente Solid State Technology), designed specifically for the optical diagnostics of the plasma plume. A schematic view of the setup is shown in figure 1. The plasma plume is generated by irradiating the target with laser pulses generated by a KrF excimer laser (248 nm, 30 ns duration FWHM, operating at 2 Hz). Using a mask placed in the KrF laser beam, a spatially uniform beam, with a cross section of $4\times15\,\mathrm{mm}^2$ and demagnified by a factor of 6.21, is incident onto the target at a 45° angle of incidence. This results in a laser spot of $0.91\times2.42\,\mathrm{mm}^2$. The laser fluence is kept at $1.3\pm10\%\,\mathrm{J/cm}^2$ during all measurements. To prevent local heating and drilling, the LAO ablation targets are mounted on a rotating holder. The deposition chamber, with a base pressure of $2\cdot10^{-7}$ mbar, is filled with either oxygen gas (99.9999%) or argon gas (99.999%).

Detection of both the spontaneous emission, by which we designate the emission of the hot plasma plume, and the LIF is done with an intensified charge coupled device (iCCD) camera, equipped with a fused silica imaging system to allow for UV imaging. During the LIF detection of AlO, a colored glass band-pass filter (275–375 nm) is used to suppress most of the spontaneous emission. For Al detection, a more narrowband interference filter of 307 ± 5 nm is used. To further

2013 JINST 8 C10021

reduce the spontaneous emission in the LIF measurements, a background subtraction (a measurement with the LIF beam turned off) is applied to all LIF measurements.

The gating time of the camera intensifier is used as shutter. The gating time for the LIF measurements is set to 44 ns, which is found to be the shortest time to still include almost all of the fluorescent decay. For the spontaneous emission measurements, the gating time is adjusted for maximum signal without saturating the camera, which is 120 ns at the longest delay times after the target ablation. All LIF images are averaged over 20 to 30 shots, depending on the signal strength, to increase the signal-to-noise ratio. The LIF lasers and iCCD camera are synchronized to the ablation laser operating at 2 Hz.

To image the neutral aluminum, we use an excitation of the atomic ground state transition at 308.2153 nm ($3s^2 3p\ ^2P^{\circ}\ ^1/_2 \rightarrow 3s^2 3d\ ^2D\ ^3/_2$). Relaxation occurs to the $3s^2 3p\ ^2P^{\circ}\ ^3/_2$ state via fluorescence at 309.2839 nm [16]. The excitation of aluminum oxide is done using the $X^2\Sigma \rightarrow C^2\Pi$ transition at 302.16 nm and detecting the red-shifted fluorescence between 303 and 306 nm [17].

The excitation wavelengths are generated by a dye laser pumped with the second harmonic (532 nm) output of a Q-switched Nd:YAG laser (7 ns FWHM). By frequency doubling the output of Rhodamine 640, both UV excitation wavelengths (6 ns FWHM, 30 pm bandwidth, 0.14 mJ) can be produced with tuning of the dye laser. To image a cross section of the ablation plume, the laser beam is transformed into a thin sheet. This is done with the combination of a cylindrical and a spherical lens, allowing for expansion in the xz-plane to a width of 35 mm (50 mm along the z-axis due to the 45° incidence angle), while the sheet is focused to approximately 0.5 mm thickness. Both lasers and the camera are triggered using a cascaded chain of delay generators.

3 Results

To investigate the oxidation of the plasma plume, we use LIF to map the spatio-temporal distribution of neutral aluminum atoms as well as neutral aluminum oxide molecules in the ground state. The location and density of both species is mapped in both oxygen and argon backgrounds.

Figure 2 shows a typical result of these measurements, at a delay of 10 μs between ablation and detection. For a direct comparison of the Al vs. AlO distribution (figure 2.1) and the AlO LIF vs. the spontaneous emission (figure 2.2), respectively, we have plotted next to each other the according half-images. Since in each single measurement the maximum is normalized to unity, the density maps cannot be compared in terms of absolute density. However, the relative distributions are well quantified.

In figure 2.1 the LIF of Al is compared to that of AlO. At the delay of 10 μs, the plasma plume has expanded several tens of mm's and the velocity of the Al atoms is reduced such by collisions with the O_2 background that they react. AlO is preferentially formed at the edges of the plume where the atoms are in direct contact with the O_2.

Figure 2.2 shows the LIF image of AlO next to the spontaneous emission which is measured without any filtering. The density distribution of AlO (figure 2.2a) is not represented in the image of the spontaneous emission (figure 2.2b), nor is the density distribution of Al (figure 2.1b). This underlines that OES is not suited for the mapping of populations in the plasma plume.

The relative densities of Al and AlO in the ground state are presented in figure 3 as function of distance from the ablation target at different delay times from ablation and in different background

2013 JINST 8 C10021

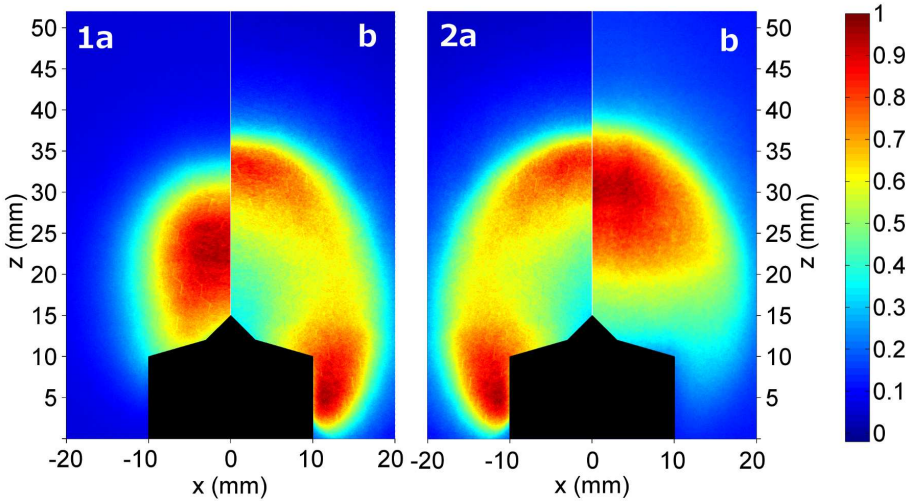

Figure 2. Images of LIF (1a, 1b & 2a) and of spontaneous emission (2b) of an LAO plasma plume versus the x and z cross section coordinates of the plume as in figure 1. Z = 0 corresponds to the surface of the ablation target. All measurements are done in $1 \cdot 10^{-1}$ mbar O_2 background pressure and at 10 μs delay from ablation. 1a) LIF of Al in O_2. 1b & 2a) LIF of AlO in O_2. 2b) Spontaneous emission in O_2. The lower part of the image is blackened because in this region the laser induced fluorescence and spontaneous emission is obstructed by the target holder which is located between the target and the iCCD camera.

gasses. Figure 3a shows that aluminum oxide is formed mostly at the front of the plume, where interaction with the background gas is strongest. Conversion of atomic aluminum to aluminum oxide can also be seen in the back of the plume, as the concentration of Al in figure 3b decreases in time, whereas the density of AlO increases (figure 3a). The absence of aluminum in the front of the plume suggests that all ground-state Al oxidizes in this region.

The same measurements in Ar instead of O_2 (figure 3c) show a clear difference in oxidation. More Al is present in Ar compared to O_2 which spreads out more over the entire plume, including the front. AlO is not present in Ar in detectable quantities (plotted at the bottom of figure 3a).

Measurements have been done on Al and AlO LIF in lower background pressures ($1 \cdot 10^{-2}$ and $1 \cdot 10^{-3}$ mbar), but our setup was unable to detect AlO due to the LIF signal being too small to measure. The spontaneous emission that is transmitted by the detection filter, which increased at lower background pressures, was one of the reasons for the decreasing detectability of AlO. However, we did see a similar absence of Al in the front of the plume in O_2 compared to Ar. This suggests that oxidation of Al is still taking place in the front of the plume.

4 Discussion & conclusions

We have applied laser induced fluorescence to measure the relative ground state densities of aluminum and aluminum oxide in the plasma plume of pulsed laser ablated $LaAlO_3$. The oxidation of aluminum has been mapped spatially and temporally in an oxygen background of $1 \cdot 10^{-1}$ mbar. Oxidation of Al in the front of the plume has been observed, where direct mixing of the plasma with the background gas takes place. Oxidation of ground state Al also takes place in the center of

2013 JINST 8 C10021

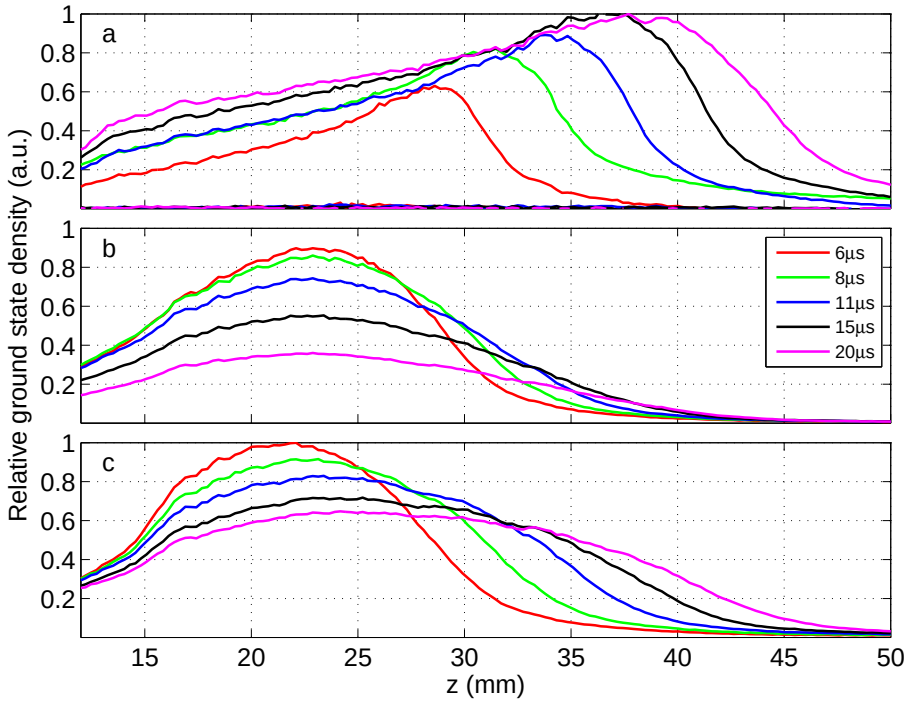

Figure 3. Relative ground state population densities of AlO (a) and of Al (b & c) along the propagation axis as function of the distance from the target at different delay times. Graphs a & b represent measurements done in an O_2 background, graph c is in Ar. All measurements are done in $1{\cdot}10^{-1}$ mbar background pressure. The relative densities of Al in graphs b & c can be compared.

the plume, but at a lower rate. An increase in Al density together with the absence of AlO in Ar confirms that aluminum is indeed oxidizing. The absence of Al in the front of the plasma plume in O_2 compared to Ar, which was visible at all three pressures ($1 \cdot 10^{-1}$, $1 \cdot 10^{-2}$ and $1 \cdot 10^{-3}$ mbar) suggest that oxidation still takes place at these settings, but at a lower rate. This would support the observations of increased oxygen vacancies in the boundary layer between STO and LAO at lower background pressures.

For future work we will increase the sensitivity of our setup to improve the AlO LIF measurements at lower oxygen pressures. We are currently working on an absolute calibration of the LIF via absorption spectroscopy, which will allow us to map densities and flows of absolute values. The latter is the key for comparison with plasma expansion models that are currently being developed.

Acknowledgments

This research is supported by the Dutch Technology Foundation STW, which is part of the Netherlands Organization for Scientific Research (NWO) and partly funded by the Ministry of Economic Affairs (project number 10760).

2013 JINST 8 C10021

References

[1] R. Eason, *Pulsed laser deposition of thin films: applications-led growth of functional materials*, John Wiley & Sons, Hoboken, U.S.A. (2007).

[2] A. Ohtomo and H.Y. Hwang, *A high-mobility electron gas at the $LaAlO_3/SrTiO_3$ heterointerface*, *Nature* **427** (2004) 6973.

[3] M. Huijben, A. Brinkman, G. Koster, G. Rijnders, H. Hilgenkamp and D.H.A. Blank, *Structure-property relation of $SrTiO_3/LaAlO_3$ interfaces*, *Adv. Mater.* **21** (2009) 1665.

[4] N. Reyren et al., *Superconducting interfaces between insulating oxides*, *Science* **317** (2007) 1196.

[5] A. Brinkman et al., *Magnetic effects at the interface between non-magnetic oxides*, *Nat. Mater.* **6** (2007) 493.

[6] A. Kalabukhov, R. Gunnarsson, J. Börjesson, E. Olsson, T. Claeson and D. Winkler, *Effect of oxygen vacancies in the $SrTiO_3$ substrate on the electrical properties of the $LaAlO_3/SrTiO_3$ interface*, *Phys. Rev. B* **75** (2007) 121404.

[7] W. Siemons et al., *Origin of charge density at $LaAlO_3$ on $SrTiO_3$ heterointerfaces: possibility of intrinsic doping*, *Phys. Rev. Lett.* **98** (2007) 196802 .

[8] G. Herranz et al., *High mobility in $LaAlO_3/SrTiO_3$ heterostructures: origin, dimensionality, and perspectives*, *Phys. Rev. Lett.* **98** (2007) 216803.

[9] C. Aruta, S. Amoruso, R. Bruzzese, X. Wang, D. Maccariello, F. Miletto Granozio and U. Scotti di Uccio, *Pulsed laser deposition of $SrTiO_3/LaGaO_3$ and $SrTiO_3/LaAlO_3$: Plasma plume effects*, *Appl. Phys. Lett.* **97** (2010) 252105.

[10] A. Sambri et al., *Plasma plume effects on the conductivity of amorphous-$LaAlO_3/SrTiO_3$ interfaces grown by pulsed laser deposition in O_2 and Ar*, *Appl. Phys. Lett.* **100** (2012) 231605.

[11] S. Amoruso, C. Aruta, P. Aurino, R. Bruzzese, X. Wang, F. Miletto Granozio and U. Scotti di Uccio, *Oxygen background gas influence on pulsed laser deposition process of $LaAlO_3$ and $LaGaO_3$*, *Appl. Surf. Sci.* **258** (2012) 9116.

[12] H.F. Döbele, T. Mosbach, K. Niemi and V. Schulz-von der Gathen, *Laser-induced fluorescence measurements of absolute atomic densities: concepts and limitations*, *Plasma Sources Sci. Technol.* **14** (2005) S31.

[13] T. Okada and M. Maeda, *Laser spectroscopic studies of pulsed-laser deposition process for high-T_c thin films*, *Mat. Sci. Eng. B-Solid* **47** (1997) 64.

[14] C. Dutouquet and J. Hermann, *Laser-induced fluorescence probing during pulsed-laser ablation for three-dimensional number density mapping of plasma species*, *J. Phys. D. Appl. Phys.* **34** (2001) 3356.

[15] Y. Nakata, T. Okada, M. Maeda, S. Higuchi and K. Ueda, *Effect of oxidation dynamics on the film characteristics of Ce:YIG thin films deposited by pulsed-laser deposition*, *Opt. Laser. Eng.* **44** (2006) 147.

[16] A. Kramida, Yu. Ralchenko, J. Reader and NIST ASD Team (2012), *NIST Atomic Spectra Database (ver. 5.0)*, National Institute of Standards and Technology, Gaithersburg, MD, U.S.A., http://physics.nist.gov/asd (30 August 2013).

[17] R.W.B. Pearse and A.G. Gaydon, *The identification of molecular spectra*, Chapman and Hall, London, U.K. (1976).

2013 JINST 8 C10021